Structural Engineering and Mechanics, *Vol. 49, No. 6 (2014) 687-703*
DOI: http://dx.doi.org/10.12989/sem.2014.49.6.687

Vibration control of 3D irregular buildings by using developed neuro-controller strategy

Yasser Bigdeli[1a], Dookie Kim[*1] and Seongkyu Chang[2b]

[1]*Department of Civil Engineering, Kunsan National University, Jeonbuk, Korea*
[2]*TE Solution Co., Ltd, Gongdo-Eup, Anseong-Si, Gyunggi-Do, Korea*

(Received September 4, 2012, Revised January 19,2014, Accepted February 1, 2014)

Abstract. This paper develops a new nonlinear model for active control of three-dimensional (3D) irregular building structures. Both geometrical and material nonlinearities with a neuro-controller training algorithm are applied to a multi-degree-of-freedom 3D system. Two dynamic assembling motions are considered simultaneously in the control model such as coupling between torsional and lateral responses of the structure and interaction between the structural system and the actuators. The proposed control system and training algorithm of the structural system are evaluated by simulating the responses of the structure under the El-Centro 1940 earthquake excitation. In the numerical example, the 3D three-story structure with linear and nonlinear stiffness is controlled by a trained neural network. The actuator dynamics, control time delay and incident angle of earthquake are also considered in the simulation. Results show that the proposed control algorithm for 3D buildings is effective in structural control.

Keywords: neural network; nonlinear control; active control; regular and irregular building

1. Introduction

Response reduction of civil structures during severe earthquakes has become a main topic in structural engineering to prevent civil structures from significant damage. One issue in seismic response control which has rarely been studied to a large extent is torsionally coupled response in 3D irregular full scale structures considering earthquake arbitrary direction. Over the past two decades, many of researches have been conducted on the development and implementation of active, semi-active, passive and hybrid control of structures (Masri *et al.* 1982, Miller *et al. 1988*, Yang *et al.* 1992, Kim *et al.* 1988), and several control strategies have been proposed, fuzzy neural network, genetic algorithm, optimal control, magnetorheological (MR) damper, sliding mode control, optimal polynomial control, equivalent passive structural control and etc., have been used extensively to reduce the response of the structures. (Agrawal and Yang 1998, Ahmadizadeh 2007, Chu *et al.* 2002, Soong 1990, Stein and Athans 1987, Ohtori *et al.* 2004, Lafontaine *et al*. 2009, Pourzeynali *et al*. 2007, Samali and Al-Dawod 2003, Sarbjeet and Datta 2003, Wang *et al*. 2009,

∗Corresponding author, Professor, E-mail: kim2kie@kunsan.ac.kr
[a]Ph.D. Candidate, E-mail: yasse.bigdeli@gmail.com
[b]Ph.D., E-mail: s9752033@gmail.com

http://www.techno-press.org/?journal=sem&subpage=8 ISSN: 1225-4568 (Print), 1598-6217 (Online)

Li *et al*. 2008, Lee and Chen 2011).

Many motivations can be mentioned for active nonlinear control structures systems development. Tall building structures need to be controlled by using active nonlinear control; in this case the linear control algorithms are not so effective subjected to severe earthquake loadings. According to displacement and torsional response of tall building structures, they may experience yielding and nonlinear action such as geometrical or material nonlinearity or both under large earthquake loadings or strong winds.

A structural damage can change the stiffness of a structure during sever dynamic loading. In this case, a numerical model supporting an assumption that the controlled structural system behave linearly would not be enough to demonstrate an actual dynamic behavior of structure. Regarding with previous researches, linear control systems cannot be effectively applied to control responses of the nonlinear span of the structural behavior (Bani-Hani and Ghaboussi 1998). Moreover, retaining a linear behavior for a large controlled structure such as a tall building in time of large earthquake loading and strong wind would need actuators with unfeasibly large capacities.

An important matter about training of a neural-network controller is to predestinate the optimal structural response for the training of a neural network controller. This should carefully be considered in a training criterion of a neural network. In most neuro-control procedures, a criterion is specified as a squared sum of offset between actual and optimal responses. An actual response can be close to the optimal responses if the criterion be minimized. Therefore, the desired structural response should be defined before the training. In the previously done researches, to eliminate the structural response a desired response is considered about equal to zero (Chen *et al*. 1995).

In many studies, different neuro-controllers based on a cost function have been proposed (Kim *et al*. 1999, Kim and Lee 2001, Kim *et al*. 2000, Lee *et al*. 2006), which were applied to a 2D building without considering irregularity of building and direction of a ground motion. In present paper, a new and simple controlling algorithm is proposed to control a 3D irregular buildings subjected to arbitrary direction of severe earthquakes. A numerical three story regular building with 3 degree of freedom (DOF) in each story is considered to evaluation of the algorithm (Fig. 3(a)). Floor diaphragms stiffness are assumed to be infinite and axial deformations of columns are zero.

2. Control algorithm

2.1 Neural network

A typical multilayer neural network is shown in Fig. 1. It has three layers including input, hidden, and output layers. According to the complexity of problems, the number of hidden layers may increase. Each layer of NN has n_1, n_2 and n_3 nodes. After receiving information by input layer at each node, the information will transfer to the nodes of hidden layer while the received information is weighted. Transferring of information from hidden layer to output layer also is in similar way and then the output of the neural network is obtained. By using trial and errors method the number of layers and nodes in each layer can be selected.

The hidden layer outputs are stated as below

$$o_i^1 = f^1(net_i^1) \quad (i = 1, 2, ..., n_2) \tag{1}$$

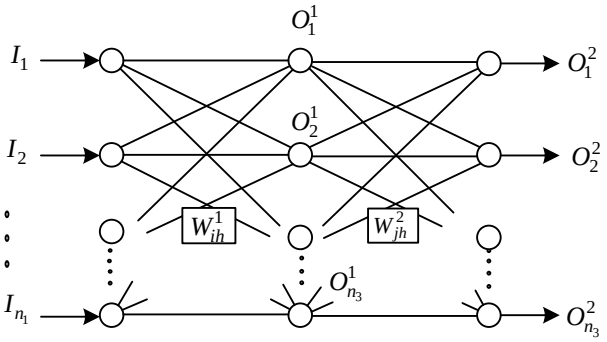

Fig. 1 Structure of multilayer perceptron with one hidden layer

inputs are denoted by I_h(h=1,2,…,n_1), and net_i^1 is a net input of the ith node of the hidden layer as follow

$$net_i^1 = \sum_{h=1}^{n1} W_{ih}^1 I_h + b_i^1 \tag{2}$$

where W_{ih}^I is the connection weight between the input and hidden layers and b_i^I is the bias of the hidden layer. The activation function of the hidden layer in Eq. (1) is presented with f^1. At the second layer the connection between two input and output net is

$$o_j^2 = f^2(net_j^2) \quad (i = 1, 2, ..., n_3) \tag{3}$$

and in this relation the net input is expressed as

$$net_j^2 = \sum_{i=1}^{n2} W_{jh}^2 o_i^1 + b_j^2 \tag{4}$$

In Eq. (4), W_{jh}^2 represents a connection weight of the hidden and output layers and b_i^2 denotes bias of the output layer.

In order to predict the required output of neural network, the weights and biases need to be defined. Training can be completed by minimizing a error criterion specified by a squared sum of the offset value between the actual and desired output of the neural network

$$E = \sum \left| o_d - o_a \right|^2 \tag{5}$$

In this relationship O_a and O_d represent the actual network output and the desired output, respectively. For making the network outputs similar to the desired output the error function must be minimized through training rule. The neural network eventually predicts the desired outputs after receiving the inputs. The network grows a controller if the desired output is control signal. But, if the desired output is not immediately accessible, the control problem depends to this case demonstrates that the training is not straight. The favorable output may be obtained to somehow apply for the error function in training. Kim *et al.* (1988, 1999), moved a proposal that in which a training algorithm is applied to the control of 2D structure. In this study, the algorithm is

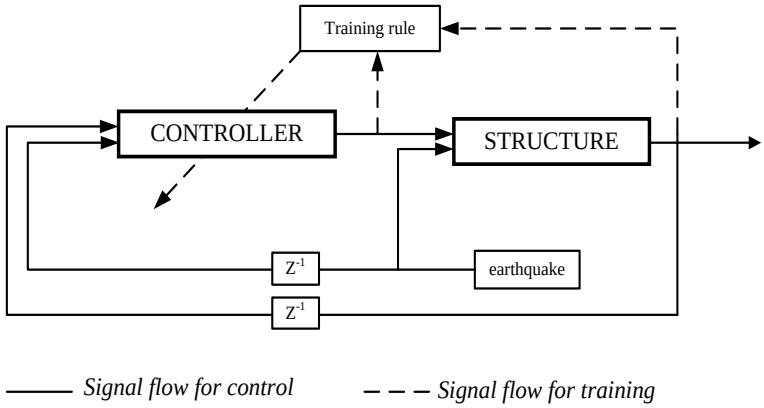

Fig. 2 Control diagram for the neuro-control

developed to train neural network controller for applying in a 3D irregular structure, and the direction of earthquake is considered as an arbitrary direction.

2.2 Algorithm for controlling system

A block diagram of the method is shown in Fig. 2 which is proposed by Kim and Lee (2001). In this procedure sensitivity is not generated by an emulator. It is obtained by an evaluation algorithm. Therefore, the emulator can be eliminated. A cost function is employed to train the neuro-controller and then determination of an optimal output is not required.

The training rule can be derived by using the cost function, combined with a structural response and a control signal is determined as

$$J = \frac{1}{2}\int_0^{T_f} (\mathbf{z}^T \mathbf{Q}\mathbf{z} + \mathbf{u}^T \mathbf{R}\mathbf{u}) dt \tag{6}$$

where $\mathbf{z}(n\times 1)$ and $\mathbf{u}(m\times 1)$ are two matrices representing the state and the control signals. $\mathbf{Q}(n\times n)$ and $\mathbf{R}(n\times n)$ denote the weighing matrices while T_f is the final time. The left-side term of the Eq. (6) refers the vibration energy and the right-side term relates to the control energy. The weighting matrices **Q** and **R** are used for making these two terms as non-dimensional term. The advantages of training by minimizing the cost function are; in this case it does not need to predetermine the desired response and at every instant both response and the control signal are extant. Moreover, the neuro-controller can be trained optimally. According to existence of mathematical model of the structure, the Riccati equation can be determined with different methods. Thus, to found the optimal control gain the equation need to be solved. As regards, it is impossible to have an optimal gain if the model has nonlinearity or some errors. Neuro-controller can control a structure by training so that it is useful in these cases. Considering the discrete-time domain the cost function can be written as follows

$$\hat{J} = \sum_{k=0}^{N_f-1} \left\{ \mathbf{z}_{k+1}^T \mathbf{Q}\mathbf{z}_{k+1} + \mathbf{u}_k^T \mathbf{R}\mathbf{u}_k \right\} = \frac{1}{2}\sum_{k=0}^{N_f-1} \hat{J}_k \tag{7}$$

where T_s, k and N_f, respectivel denote the sampling interval, the sampling number, and the total number of sampling times. The weight parameter W_{ji}^2 needs to be updated regularly, so after application of gradient descent rule to the cost function at k th step, the update for this parameter at this step is

$$\Delta W_{ji}^2 = -\eta \frac{\partial \hat{J}_k}{\partial W_{ji}^2} \tag{8}$$

where the η denotes the rate of training. The convergence of training can be modified by changing the rate of training. The partial derivative of Eq. (8) is expressed as

$$\frac{\partial \hat{J}_k}{\partial W_{ji}^2} = \frac{\partial \hat{J}_k}{\partial net_j^2} \frac{\partial net_j^2}{\partial W_{ji}^2} \tag{9}$$

the generalized error is as follow

$$\delta_j^2 = -\frac{\partial \hat{J}_k}{\partial net_j^2} - \frac{\partial \hat{J}_k}{\partial o_j^2} \frac{\partial o_j^2}{\partial net_j^2} \tag{10}$$

the weight update is as below

$$\Delta W_{ji}^2 = \eta \delta_j^2 \mathrm{o}_\mathrm{i}^1 \tag{11}$$

where

$$\delta_j^2 = -\left(z_{k+1}^T Q \left\{ \frac{\partial \mathrm{z}_{k+1}}{\partial u_{k,j}} \right\} + u_k^T r_j \right) \mathrm{G_j}(f^2)' \Big|_{\mathrm{net}_\mathrm{j}^2} \tag{12}$$

In this relationship, the gain factor, G_j convinces

$$u_j = G_j o_j^1 \tag{13}$$

in which, r_j is the jth column vector of **R**. The bias can be updated by

$$\Delta b_j^2 = \eta \delta_j^2 \tag{14}$$

According to that all the terms are available at the kth step In Eq. (12), in the same procedure, update for the weight, W_{ji}^1 is determined as

$$W_{ji}^1 = \eta \delta_j^1 I_h \tag{15}$$

where

$$\delta_j^1 = -\frac{\partial \hat{J}_k}{\partial net_j^1} = -\sum_{j=1}^{n3} \frac{\partial \hat{J}_k}{\partial net_j^2} \frac{\partial net_j^2}{\partial o_i^1} \frac{\partial o_j^1}{\partial net_j^1} = \sum_{j=1}^{n3} \delta_j^2 W_{ji}^2 (f^1)' \Big|_{net_i^1} \tag{16}$$

and the update for the bias of the hidden layer is as below

$$\Delta b_i^1 = \eta \delta_i^1 \tag{17}$$

3. Structural model

3.1 Nonlinear dynamics of 3D model

A real building structure can normally have both plan and elevation irregularities. Generally, in the real structures the center of mass (CM) is not at the same point with the center of resistance (CR) in each floor. The location of centers of mass and resistance of floors can change from floor to floor due to different story stiffness's along with the two main directions so that they do not lie on the same vertical line. This difference can happen for a structure with even a symmetric plan because different members with different stiffness may be used in a symmetric floor ordering. In these kinds of conditions there is an interaction between lateral and torsional behaviors which normally underestimates the maximum structural responses under a dynamic excitation (Kim and Lee 2001).

In present paper, floor diaphragms are considered to be rigid and axial displacements of columns are zero. In this way, a building model is created using three displacement degrees of freedom (DOF) at each rigid floor: there are two translation components in *x*- and *y*- directions and a rotation about the vertical axis *z* passing through the center of resistance (CR). Therefore, sum of the DOFs is equal to n=3 m, where m is the number of stories. The structural displacement response at time t is stated as

$$u(t) = \left[u_1(t)\ u_2(t) \ldots u_m(t)\ v_1(t)\ v_2(t) \ldots v_m(t)\ \theta_1(t)\ \theta_2(t) \ldots \theta_m(t)\right]^{\mathrm{T}}_{3\mathrm{m}\times 1} \tag{18}$$

where $u_i(t)$ and $v_i(t)$ respectively denote the displacements in *x*- and *y*- directions. $\theta_i(t)$ is the rotation about the vertical axis *z* of the *i*th floor and '*T*' denotes the transpose of the matrix. The equation of motion of 3D model with an active control system installed on the roof subjected to an earthquake excitation is stated as

$$\mathbf{M}\ddot{u}(t) + \mathbf{C}\dot{u}(t) + \mathbf{R}(x,t) = \mathbf{I}_c F(t) - \mathbf{M}_0 I_g \ddot{x}(t) \tag{19}$$

In this Equation *M* and *C* respectively denote $n\times n$ mass and damping coefficient matrices of the structure; $\mathbf{R}(x,t)$ is the $n\times 1$ restoring force vector; $F(t)$ is the $n\times 1$control force vector that components of $F(t)$ are in the form of time series; I_c is an $n\times n$ location matrix representing the location of the actuators; and $\ddot{x}_g$ is the input horizontal earthquake acceleration with arbitrary orientation. In present research, it is assumed that two pairs of actuators are applied in AMD system in the roof along with two main perpendicular axes, *x* and *y* (Fig. 3(b)). Each pair has two same actuators representing the control force $F(t)$ in the corresponding direction. To minimize the moment caused by actuators in two directions, a proper assigning of the control force to the two actuators in each direction is required. In order to simplify the computations; the distance between the center of mass (C_M) and the centre of resistance (C_R) in each floor is neglected. Therefore, at roof level where the actuators are installed; moment caused by actuators in two directions is ignored. The actuators are installed in two orientations as δ=0° (parallel to *x*- axis) for one pair and δ=90° (perpendicular to *x*- axis) for another pair.

In Eq. (19), M_0 and I_g are a $n\times n$ diagonal mass matrix and an $n\times 1$ orientation matrix denoting

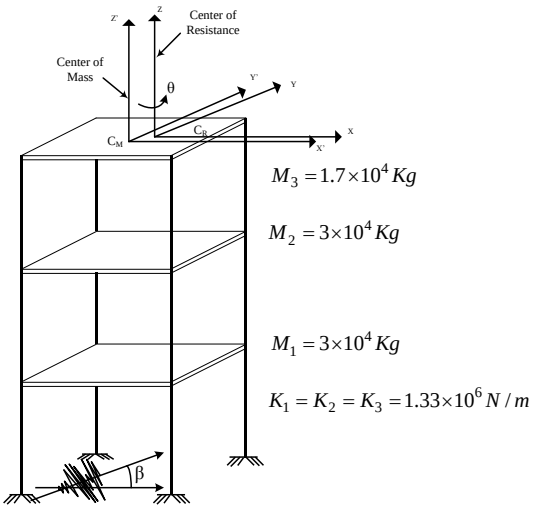

(a) Seismic excitation applied with arbitrary angle

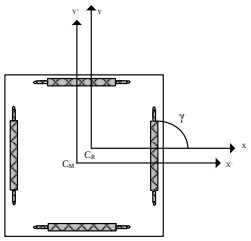

(b) Actuators in top story

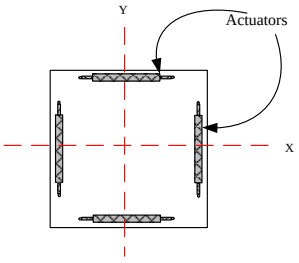

(c)

Fig. 3 Three story 3-D building model: (a) 3-D building structure and (b) Plan of the top story with two pairs of actuators

the orientation of the external seismic excitation, in order. I_g can be written as below

$$I_g = [\cos(\beta)\ \cos(\beta)\ \cos(\beta)\ \cos(\beta)...\ \sin(\beta)\ \sin(\beta)\ \sin(\beta)\ \sin(\beta)...0\ 0\ 0\ 0...] \tag{20}$$

while β indicates an arbitrary direction angle of earthquake excitation scale from the *x*- axis as it shown in Fig. 3(a).

A building structure installed with an active control system at roof level is shown in Fig. 3. When the structure is exposed to an earthquake excitation, represented by the horizontal ground acceleration in the form of a time series, the response of structure at the roof, such as $u(t)$ in the *x*-direction, can be sent to the controller along with the earthquake excitation vector. Proper control forces obtained by the actuators can minimize the structural displacement at the top floor of the structure in all the time steps. The actuator properties are base to convert each control force to a corresponding control signal; the actuators are excited according to the control signal to generate the required control force.

3.2 Hydraulic actuator

The previous researches (Bani-Hani and Ghaboussi 1998, Lee *et al.* 1998) have recognized that the actuator-structure interaction in active control of structures is quite important. In present study, in order to active control of a building a linear hydraulic actuator is employed. This controlling system is used to create rather large forces with a small response time (Nikzad *et al.* 1996). The magnitude of generated force by a hydraulic actuator can be as 1,000 kN.

The four double-acting actuators with the same properties are installed in top floor as presented in Fig. 3(c).

To cover the equation of motion of hydraulic actuator properly, it need to be derived in two equations, the valve dynamics and the piston equation.

The valve equation of actuator is as follows

$$\frac{\tau}{g}\dot{q}+\frac{1}{g}q=u \tag{21}$$

where g and τ represent the servovalve constant and the time constant of the valve. q and u respectively are the flow rate of the oil and the control signal. The valve compels the motion of the piston with changing of the oil flowing rate. The relevant equation is derived as

$$a_r\dot{x}_r+\frac{c_l}{a_r}f+\frac{v}{2c_c a_r}\dot{f}=q \tag{22}$$

where a_r and V represent the area of piston and the volume of the cylinder; x_r the relative displacement between the roof and the piston. c_c and c_l are the compressibility coefficient and leakage coefficient; f is the force applied to the structure by the AMD system (Dyke *et al.* 1995, DeSilva 1989).

3.3 Nonlinear dynamic model

In order to simulate the motion of nonlinear structure, a nonlinear model suggested by Baber and Wen (1981) is used. This model is successfully applied to the control simulations in the several researches (Bani-Hani and Ghaboussi 1998). A model, combination of linear and nonlinear terms, for restoring force is introduced as

$$k_s(x_s,\dot{x}_s)=\alpha k_0 x_s+(1-\alpha)k_0 d_y y \tag{23}$$

where x_s is the displacement of element, $\alpha k_0 x_s$ and $(1-\alpha)k_0 d_y y$ represent the linear and nonlinear divisions of the restoring force, respectively. k_0 and αk_0 ($\alpha<1$), respectively, denotes the slope coefficients for linear and nonlinear divisions of the load-displacement curve (Fig. 4); and y represents a hysteretic variable. The following differential equation expresses the hysteretic variable in the range $-1\leq y\leq 1$, as follows

$$\dot{y}=\frac{1}{d_y}(\rho\dot{x}_s-\mu|\dot{x}_s||y|^{p-1}-\sigma\dot{x}_s|y|^p) \tag{24}$$

where ρ, μ and σ indicate the constants which change the hysteretic behavior of model.

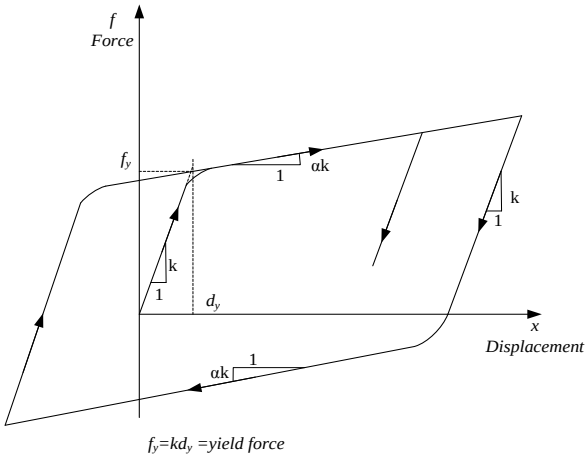

Fig. 4 Force-displacement graph of an element with material nonlinearity (Jiang and Adeli 2008)

Table 1 Properties of the actuator

Variables	Description	value
a_r	Area of piston	3.368×10^{-3} m^2
v	Volume of the cylinder	1.01×10^{-3} m^3
c_l	Leakage coefficient	0.1×10^{-10} m^5/(Ns)
c_c	Compressibility coefficient	2.1×10^{10} N/m^2
$q_{\max}$	Maximum flow rate of oil	2.0×10^{-3} m^3/s
τ	Servovalve time constant	0.15 Sec
g	Servovalve constant	2.1×10^{-4} m^3/s/*volt*

4. Results and discussion

4.1 Numerical model

The structural properties are as follows: according to ACI (2005) code provisions, the calculated masses of the first, second and third story are 3×10^4, 3×10^4 and 1.7×10^4 Kg, respectively; 8×10^4, 8×10^4, 4.533×10^4 Kg.m^2 are the moment of inertia for diaphragm in the first, second and third floors; moreover the inter-story stiffness in two x- and y-directions, for all stories is 1.33×10^6 N/m (Fig. 3); Damping matrix is calculated by using the Rayleigh damping method as follows

$$\mathbf{C} = a_1\mathbf{M} + a_2\mathbf{K} \tag{25}$$

where a_1 and a_2 have units of sec^{-1} and sec, respectively. The sampling time is 0.005s, delay time is assumed to be 0.0005s. The equation of motion is integrated at every 0.00025s; using Matlab 2008a. The properties of an actuator used in this study are based on data provided by one manufacturer (http://www.mts.com) and are summarized in Table 1 (Jiang and Adeli 2008).

Time delay is inevitable in implementation of a controller. It is caused by computation of the control signal that is applied to the actuator. At the *k*th step of sampling time, the state of structure,

z_k is identified and used as a feedback signal to compute the control signal. Although it is short, computation of the control signal can take time. Thus the control signal is not applied at the time kT_s but at the time kT_s plus the delayed time. If the time delay is not considered in the design, the performance of the controller may be worse than expected. Hence, the effect of time delay should be considered.

4.2 Training the controller

In this study employed neuro-controller includes three layers. The input layer, as first layer, has nine nodes that in which the feedback signals of the displacement, velocity of third floor and the ground acceleration in *x*, *y*, and θ (rotation) directions are supported. The hidden layer, as second layer, also has nine nodes. The third layer, called output layer, has three nodes which produce control signal in special three directions. The sigmoid function is considered as the activation function of the second layer and the linear function for the third layer. Normalized state of third floor is used to the uncontrolled responses participates in the cost function.

The cost function employed for training criterion at the *k*th step is expressed as

$$\hat{J}_k = \mathbf{z}_{3,k+1}^T \mathbf{Q} \mathbf{z}_{3,k+1} + r u_k^2 \tag{26}$$

The weighting matrix *Q* and *r* are expressed as

$$\mathbf{Q} = \begin{pmatrix} \left|\frac{1}{\tilde{x}_3}\right|^2 & 0 \\ 0 & \left|\frac{1}{\dot{x}_3}\right|^2 \end{pmatrix} \tag{27}$$

$$r = 0.1\left|\frac{1}{\tilde{u}}\right|^2 \tag{28}$$

In Eq. (26), $\mathbf{z}_{3,k+1}^T$ and u_k respectively denote the state of third floor and control signal. The value of 0.1 is calculated by using a trial and error procedure to reach the optimal energy response.

In these Eqs. (27) to (28), $\tilde{x}_3$ and $\dot{x}_3$ represent the maximum displacement and velocity of third floor under the earthquake excitation when control input is off. The maximum control input voltage is denoted by $\tilde{u}$. El-Centro earthquake record (1940) is employed as an earthquake excitation with peak ground acceleration (PGA) 0.348g. Two-thousand time intervals among the dynamic responses under this specific excitation are employed for training data.

4.3 Control results

Controlled and uncontrolled displacement responses of the model under three earthquake loads: El-Centro, Northridge and California (Fig. 5) are determined. The modal analysis of the structure demonstrates that the coupling effect of lateral and torsional vibration will be significant for an irregular structure when the earthquake excitation is applied in a suitable direction β.

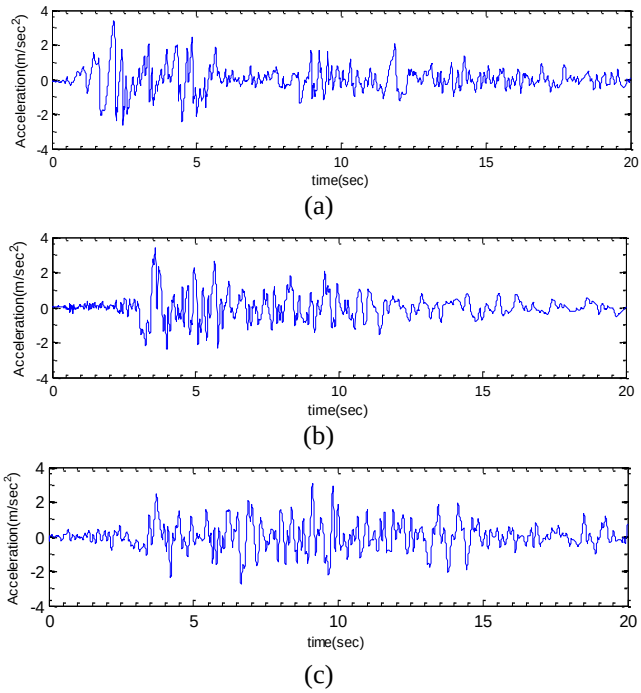

Fig. 5 (a) El-Centro earthquake used for training (b) Northridge earthquake (c) California earthquake

Table 2 Maximum displacements of top floor of 3-story structure subjected to three earthquake ground accelerations

Earthquake	Displacement response	Uncontrolled(m)	Controlled(m)	Reduction (%)
Northridge	*X*	0.0375	0.0114	69.49
β=45°	*Y*	0.0375	0.0114	69.49
Northridge	*x*	0.0433	0.016	63.053
β=30°	*y*	0.02108	0.00708	66.39
El-Centro	*x*	0.0351	0.0079	77.415
β=45°	*y*	0.0351	0.0079	77.415
El-Centro	*x*	0.0412	0.0080	80.50
β=30°	*y*	0.0240	0.0075	68.403
California	*x*	0.039	0.0106	72.67
β=45°	*y*	0.039	0.0106	72.67
California	*x*	0.0441	0.0143	67.42
β=30°	*y*	0.0236	0.00864	63.35

The El-Centro earthquake with the direction angle of earthquake excitation β=45°, is applied to train control algorithm. Results are showing that displacement, velocity and acceleration are decreased considerably in controlled structure. In Fig. 8 it is shown that by controlling the structure the total modal energy are decreased significantly in all cases. Results of controlled and uncontrolled displacement response in two principle directions *x* and *y*, for Northridge, El-Centro

Table 3 Maximum displacements of the top floor of the 3-story structure subjected to three earthquake ground accelerations

Earthquake	Beta	Uncontrolled(m)	Controlled (m)	Reduction (%)
Northridge	0	0.0533	0.0161	69.79
	90	0.0533	0.0161	69.79
El-Centro	0	0.0496	0.0111	77.62
	90	0.0496	0.0111	77.62
California	0	0.0551	0.0149	72.95
	90	0.0551	0.0149	72.95

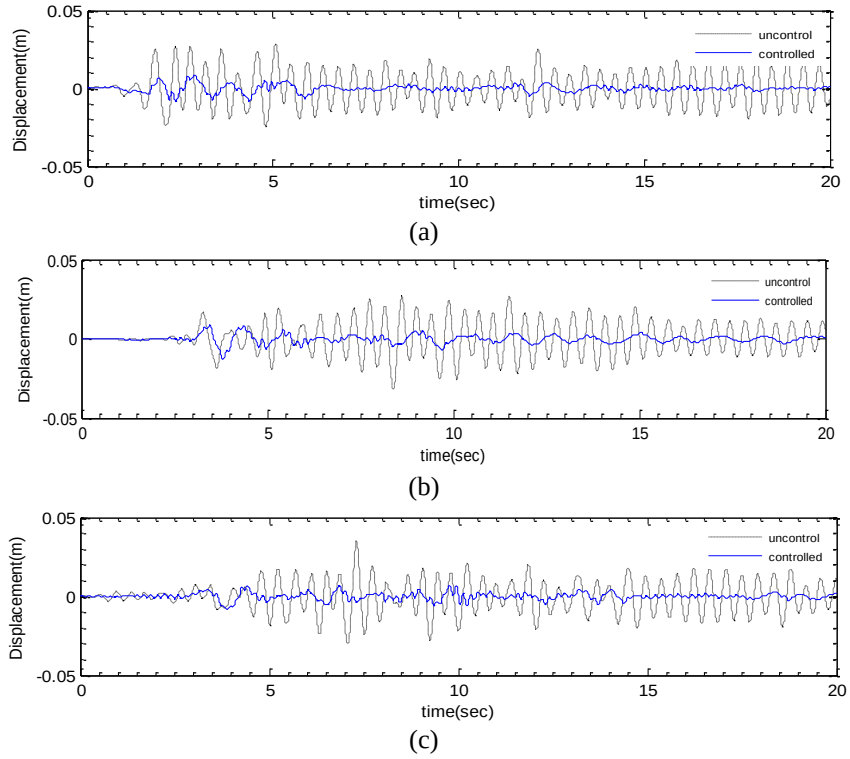

Fig. 6 Uncontrolled and controlled displacement response of third floor of structure under (a) El-Centro earthquake acceleration, (b) Northridge earthquake acceleration, (b) California earthquake acceleration, in *x*- direction when β=45°.

and California earthquakes are presented in Figs. 6, 7. All the excitations are applied in two directions β=30° and β=45°. Percentage of decreasing in displacement responses are shown in Table 2. Table 2 presents maximum displacement of the top floor of a three story structure subjected to three earthquake ground accelerations. In all cases two directions β=45° and 30° are selected for application of earthquake excitations. The structural model is perfectly regular, and β is 45°, so the responses of structure in two principle x- and y- directions are same, and in case of β=30° they should be different. In addition to this, Table 3 provides some results for the structure subjected to the above mentioned ground motions when β=0°, 90° for comparison purpose. It is

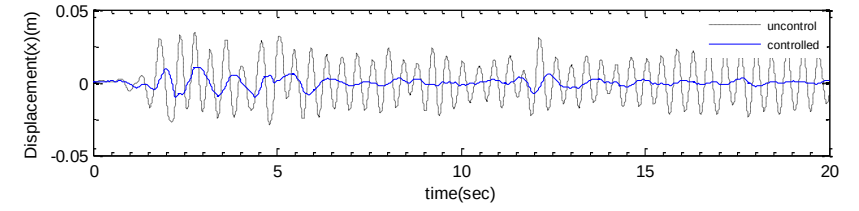

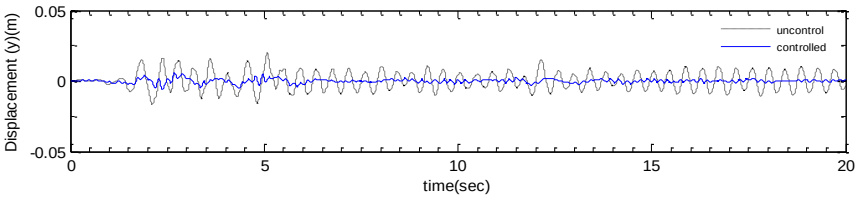

(a) El-Centro

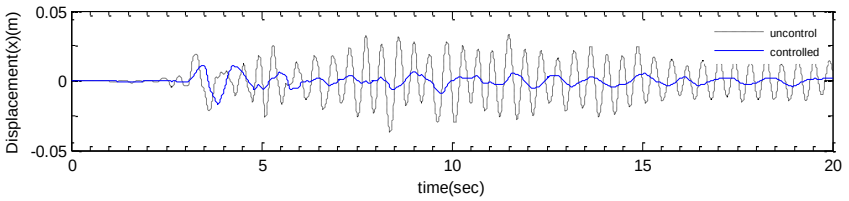

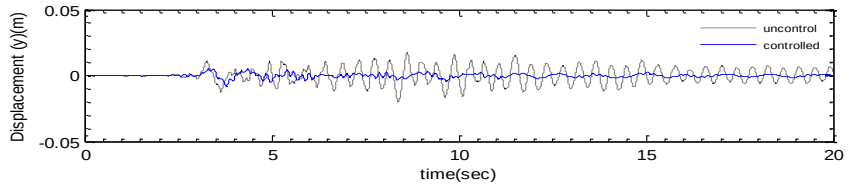

(b) Northridge

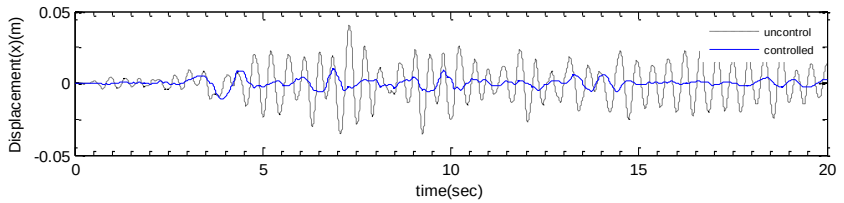

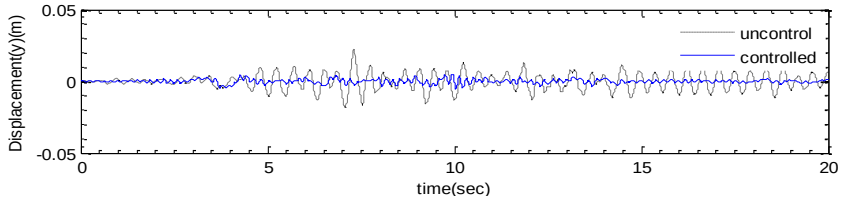

(c) California

Fig. 7 Uncontrolled and controlled displacement response of the third floor of the structure under (a) El-Centro, (b) Northridge and (C) California earthquake acceleration in *x*- and *y*- direction when β=30°

obvious that results for these directions should be the same as it is listed in the table, because the structural model is perfectly regular.

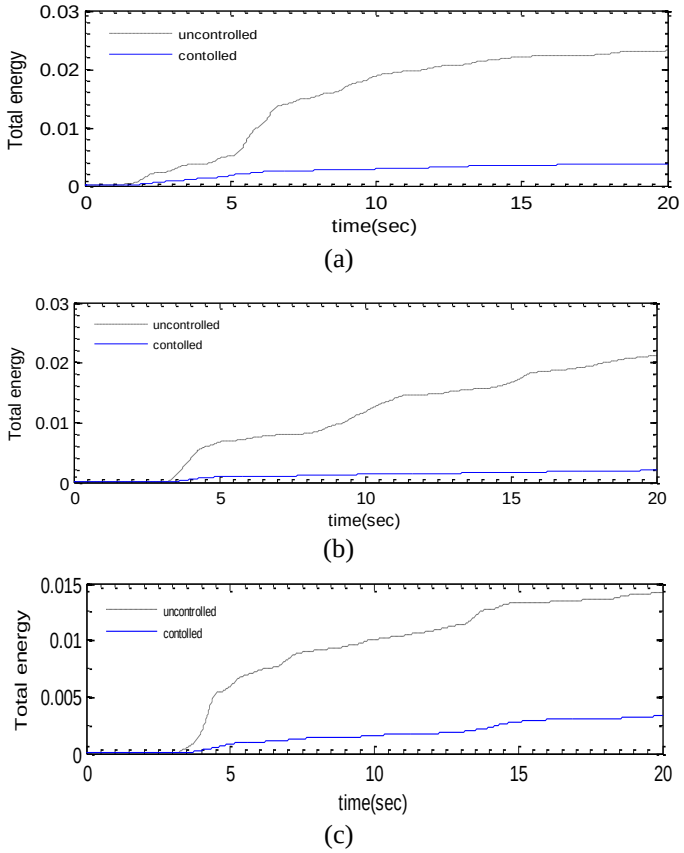

Fig. 8 Modal energy of the controlled and uncontrolled structure under (a) El-Centro, (b) Northridge, (c) California earthquake, When β=45°

The maximum reductions occurred in the displacement response of the top floor of the structure after application of the control algorithm for β=45° are: 69.49, 77.415 and 72.67 percent for Northridge, El-Centro and California earthquakes, respectively. The maximum reduction for El-Centro earthquake is 80.50% in the *x*-direction when β=30° while the minimum response reduction in the same direction β for Northridge ground motion is 63.05 %. To clarify the difference for two cases, it should be considered that the maximum reduction happens for the structure subjected to El-Centro ground motion by which the controller is trained. It determines that the algorithm is more effective for the structures subjected to the dynamic excitation signal by which the controller is trained. Nevertheless, for the rest of cases the difference is not significantly noticeable.

The restoring force in the *x*-direction, for controlled and uncontrolled structure for β=45°, is determined under different earthquake excitations. In Fig. 9 the restoring forces of the controlled and uncontrolled structure are shown, figures on the left columns are uncontrolled, and ones on the right columns are restoring force of the controlled structure.

In this study, the control algorithm is organized to control of 3D irregular buildings subjected to an arbitrary direction of an earthquake, while in the prior researches (Kim *et al.* 1999, Kim *et al.* 2000), the algorithms are used to control a 2D structure. Irregularity of structure and direction of the earthquake load are also not considered in mentioned researches.

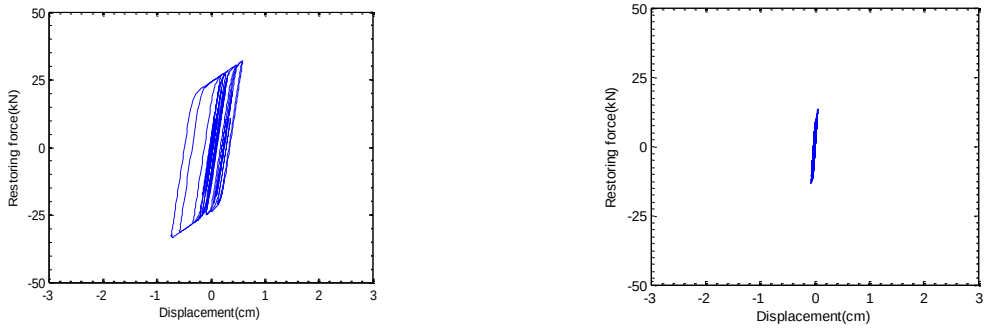

Third floor- El-Centro earthquake

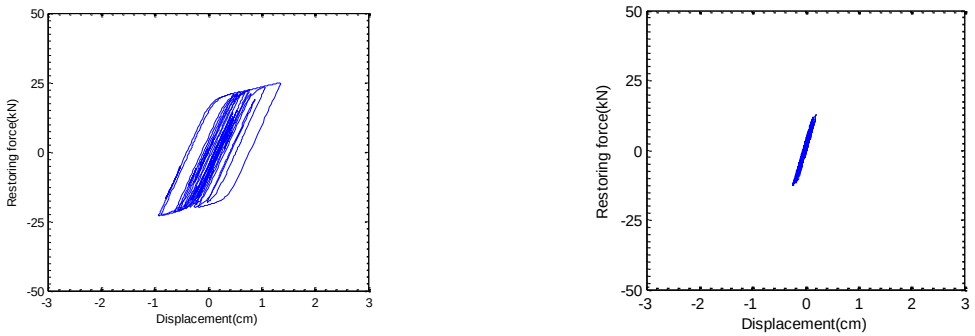

Third floor- Northridge earthquake

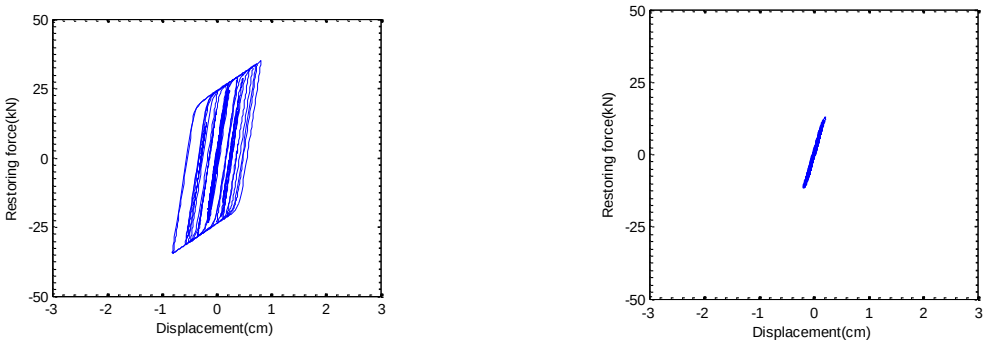

Third floor- California earthquake

Fig. 9 Restoring force versus displacement (left column uncontrolled; right column controlled)

5. Conclusions

An effective algorithm is proposed to control irregular three-dimension buildings. The proposed algorithm is applied for the control a regular 3D three-story building and results look promising in structural control. A structural model has been used for the active nonlinear control of a 3D three story structure. Two dynamic motions are calculated simultaneously in the control model such as coupling between torsional and lateral responses of the structure and interaction between the structural system and the actuators. The proposed algorithm requires the installation of two pairs of actuators only at the top floor of the building to control the responses of 3D irregular structures effectively while other algorithms at least need installation of two pairs of

actuators in any floor of irregular building structures.

Acknowledgments

This work was supported by the Nuclear Research & Development of the Korea Institute of Energy Technology Evaluation and Planning (KETEP) through a grant funded by the Ministry of Knowledge Economy and by the National Research Foundation of Korea Grant funded by the Korean Government (NRF-2012S1A2A1A01030512).

References

ACI 318-05 (2005), "Building Code Requirements for Structural Concrete and Commentary", American Concrete Institute.

Agrawal, A.K. and Yang, J.N. (1996), "Optimal polynomial control of seismically excited linear structures", *J. Eng. Mech., ASCE*, **122**(8), 753-761.

Ahmadizadeh, M. (2007), "On equivalent passive structural control system for semi-active control using viscous fluid dampers", *J. Struct. Control Hlth. Monit.*, **14**, 858-875.

Baber, T.T. and Wen, Y.K. (1981), "Random vibration of hysteretic degrading systems", *J. Eng. Mech., ASCE*, **107**(6), 1069-1087.

Bani-Hani, K. and Ghaboussi, J. (1998), "Nonlinear structural control using neural networks", *J. Eng. Mech., ASCE*, **124**(3), 319-327.

Chen, H.M., Tsai, K.H., Qi, G.Z., Yang, J.C.S. and Amini, F. (1995), "Neural network for structural control", *J. Comput. Civil Eng., ASCE*, **9**(2),168-176.

Chu, S.Y., Soong, T.T., Reinhorn, A.M., Helgeson, R.J. and Riley, M.A. (2002), "Integration issues in implementation of structural control systems", *J. Struct. Control*, **9**, 31-58.

DeSilva, C.W. (1989), *Control sensors and actuators*, Prentice Hall, Inc., Englewood Cliffs, N.J.

Dyke, S.J., Spencer, B.F., Jr., Quast, P. and Sain, M.K. (1995), "Role of control-structure interaction in protective system design", *J. Eng. Mech., ASCE*, **121**(2), 322-338.

Edwards, C. and Spurgeon, S. (1998), *Sliding Mode Control: Theory and Applications*, Taylor & Francis, CRC Press, London, Boca Raton, FL.

Jiang, X. and Adeli, H. (2008), "Dynamic fuzzy wavelet neuroemulator for nonlinear control of irregular building structures", *Int. J. Numer. Method. Eng.*, **74**, 1045-1066.

Kim, D.H. and Lee, I.W. (2001), "Neurocontrol of seismically excited steel structures through sensitivity evaluation scheme", *Earthq. Eng. Struct. Dyn.*, **30**(9), 1361-1377.

Kim, J.T., Jung, H.J. and Lee, I.W. (2000), "Optimal structural control using neural networks", *J. Eng. Mech.*, **126**(2), 0733-9399.

Kim, J.T., Oh, J.W. and Lee, I.W. (1999), "Artificial neural networks for structural vibration control", *Proceedings of the 1st International Conference on Advances in Structural Engineering and Mechanics*, Seoul, August.

Lafontaine, M., Moroni, O., Sarrazin, M. and Roschke, P. (2009), "Optimal control of accelerations in a base-isolated building using magneto-rheological dampers and genetic algorithms", *J. Earthq. Eng.*, **13**(8), 1153-1171.

Lee, H.J., Yang, G., Jung, H.J. and Spencer, B.F., Jr. (2006), "Semi-active neurocontrol of a base-isolated benchmark structure", *J. Struct. Control Hlth. Monit.*, **13**, 682-692.

Lee, T.Y. and Chen, P.C. (2011), "Experimental and analytical study of sliding mode control for isolated bridges with MR dampers", *J. Earthq. Eng.*, **15**(4), 564-581.

Li, J., Peng, Y.B., and Chen, J. (2008), "GDEE-based stochastic control strategy of MR damping systems",

Proceedings of the Tenth International Symposium on Structural Engineering for Young Experts, Changsha, China.

Lu, L.T., Chiang, W.L. and Tang, J.P. (1998), "LQG/LTR control methodology in active structural control", *J. Eng. Mech., ASCE*, **124**(4), 446-454.

Masri, S.F., Bekey, G.A. and Caughey, T.K. (1982), "On-line control of nonlinear flexible structures", *J. Appl. Mech*., **49**(12), 871-884.

Mathlab (2008), "The Language of Technical Computing", Math works Inc., MA.

Miller, R.K., Masri, S.F., Dehghanyar, T. and Caughey, T.K. (1988), "Active vibration control of large civil structures", *J. Eng. Mech*., *ASCE*, **114**(9), 1542-1570.

Nikzad, K., Ghaboussi. J. and Paul, S.L. (1996), "Actuator dynamics and delay compensation using neurocontrollers", *J. Eng. Mech*., *ASCE*, **122**(3), 218-229.

Ohtori, Y., Christenson, R.E., Spencer, B.F., Jr. and Dyke, S.J. (2004), "Benchmark control problems for seismically excited nonlinear buildings", *J. Eng., Mech*., **130**(4), 366-385.

Pourzeynali, S., Lavasani, H. and Modarayi, A.H. (2007), "Active control of high rise building structures using fuzzy logic and genetic algorithms", *Eng. Struct.*, **29**(3), 346-357.

Samali, B. and Al-Dawod, M. (2003), "Performance of a five-storey benchmark model using an active tuned mass damper and a fuzzy controller", *Eng. Struct.*, **25**, 1597-1610.

Sarbjeet, S. and Datta, T.K. (2003), "Sliding mode control of building frames under random ground motion", *J. Earthq. Eng.*, **7**(1), 73-95.

Soong, T.T. (1990), *Active Structural Control: Theory and Practice*, Longman's, New York.

Stein, G. and Athans, M. (1987), "The LQG/LTR procedure for multivariable feedback control design", *IEEE Tran. Auto. Control*., **32**(2), 105-114.

Wang, Z.H., Chen, Z.Q. and Spencer, B.F., Jr. (2009), "Self-powered and sensing control system based on MR damper: presentation and application", *Proceedings of SPIE Smart Tructures/NDE*, San Diego, California.

Yang, J.N., Danielians, A. and Liu, S.C. (1992), "Hybrid control of nonlinear and hysteretic systems I&II", *J. Eng. Mech., ASCE*, **118**, 1423-1457.